

Intensity Modulated Fiber Optic Sensor: A Novel Grid Measurement Unit

Wenxuan Yao, *Senior Member, IEEE*, Lingwei Zhan, *Member, IEEE*, Sterling Rooke, Christopher Vizas, Victor Kaybulkin, Thomas J King, Bailu Xiao, *Member, IEEE*, Zhi Li, *Member, IEEE*, Yilu Liu, *Fellow, IEEE*, and He Yin, *Senior Member, IEEE*

Abstract— This paper presents a novel approach to physical displacement-based power grid measuring via an Intensity Modulated Fiber Optic Sensor (IMFOS). An IMFOS utilizes one fiber to transmit the intensity modulation light from its Electro-Optic controller to a fiber optic probe. The power grid voltage and current can induce physical displacements in transducers via the piezoelectric effect and the Lorentz law, respectively, which then result in a distance change between the optical probe and the reflective surface of the transducers. In parallel, multiple fibers are used to collect the reflective light for electro-optic conversion. A National Instruments-based characterization platform is set up for performance evaluation. The testing result demonstrates that the IMFOS is immune to the inherent DC and low-frequency saturation issues prevalent in conventional potential and current transformers. Finally, the IMFOS is implemented in a Universal Grid Analyzer to illustrate its applicability for phasor estimation in actual power grids.

Index Terms—Intensity modulated fiber optic, power grid measuring, universal grid analyzer

I. INTRODUCTION

High-fidelity monitoring devices such as Phasor Measurement Units (PMUs) play an essential role in improving the reliability and resilience of the power grid by providing real-time measurements of voltage and current [1]-[6]. As the feedback from power system actuators, precise and real-time measurements are the solid foundations and strong supports for power system automation applications such as distributed energy source controls [7], damping controls [8], power system situational awareness [9], and event localization [10]. For instance, by using the synchrophasors provided by multiple PMUs, a damping controller can mitigate major categories of frequency oscillations and allow more renewable electricity in

power grids.

Conventional electromagnetic Potential Transformers (PTs) and Current Transformers (CTs) are widely installed to provide a measurement interface for grid monitoring devices. By using both CT and PT, PMUs and the supervisory control and data acquisition systems (SCADAs) can provide real-time measurements to the grid control center. Unfortunately, such magnetic-core-based PT/CTs have inherent weaknesses, such as magnetic saturation, electromagnetic interference sensitivity, and poor linearity, which typically becomes one of the bottlenecks for reliable and accurate grid measurements [11]-[13]. For example, the DC component under the fault conditions can cause the saturation of transducers, which would have an adverse impact on the protection functions of the relay and consequently on the system stability [14]. Moreover, the conventional PT and CT require a direct physical connection to a conductor for sensing and thus, are usually equipped with oil or sulfur hexafluoride (SF₆) gas for insulation. Such specific requirements complicate their installation process and increase overall maintenance costs, especially under conditions of harsh and explosive environments [15][16]. The electric and magnetic field-based non-contact sensor was developed and tested for the synchronized measurement of a high voltage transmission line, which would dramatically reduce manufacturing and installation costs [17][18]. However, these wireless sensors lack robustness and can produce large harmonic distortions.

Applications of fiber-optic sensors can be a powerful tool for the measurement of various physical parameters [19][20]. Since fiber-optics use light rather than electricity, the fiber-optic sensor is not sensitive to Electromagnetic Interference (EMI) and thus, is superior in such applications with minimal need for dielectrics. Moreover, the optical sensors are able to address the saturation concerns inherent in existing electromagnetic CT and PT. For the application of power grid sensing, the most common approach of existing optical sensors has relied on the interaction between light and an electromagnetic field based on Faraday and Pockels effects, which rotates an optical probe field polarization state in proportion to the magnetoelectric fields and measures the changes in light phase and polarity which in turn, indicates various electric and magnetic phenomena [17]-[26]. However, the effects of light polarization, temperature, filtration calibration, and birefringence drift all adversely impact the performance of these sensors. Moreover, the specialized polarization required by components coupled with the calibration process, makes the sensor design costly to manufacture.

This work is supported by U.S. Department of Energy (DOE) under the Grid Modernization Grid Modernization Laboratory Consortium (GMLC) program.

W. Yao, L. Zhan, T. King, B. Xiao and Z. Li are with Oak Ridge National Laboratory, Oak Ridge, TN, USA 37831 (email: ywxhnu@gmail.com, zhanl@ornl.gov, kingtj@ornl.gov, xiaob@ornl.gov, liz2@ornl.gov)

Y. Liu is with the Department of Electrical Engineering and Computer Science, University of Tennessee, Knoxville, TN, 37996, USA and also with Oak Ridge National Laboratory, Oak Ridge, TN, 37831, USA (email: liu@utk.edu)

S. Rooke and H. Yin are with the Department of Electrical Engineering and Computer Science, University of Tennessee, Knoxville TN, USA, 37996 (email: srooke@utk.edu, hyin8@utk.edu)

C. Vizas and V. Kaybulkin are with SmartSenseCom, Vienna, VA, USA 22180 (email : cvizas@smartsensecom.com,

Compared with the light polarization modulation method, the Intensity Modulated Fiber Optic (IMFO) approach has merits in its simplicity and robustness [27][28]. Unlike the light polarization modulation technology, the IMFO does not require interferometry or lasers and is less susceptible to the effects of temperature and vibration. Since IMFO is a promising technology for physical parameter measurement, this paper investigates the feasibility of exploiting this technology for power grid voltage and current measurement, with the expectation to overcome the inherent weaknesses in conventional transducers. The proposed Intensity Modulated Fiber Optic Sensor (IMFOS) transmits 850 nanometer infrared light to its probes via a center fiber. Since the power grid voltage and current can induce physical displacements in transducers via the piezoelectric effect and Lorentz law, respectively, a distance change between the optical probe and the reflective surface of the transducers will occur. Meanwhile, six fibers around the center fiber are used to collect the reflective light, with strength dependent directly on the displacement caused by the physical phenomena of interest. With this in mind, a prototype of IMFOS was fabricated for 120 V/60 Hz power grid monitoring. To evaluate the performance of the prototype sensor, a characterization platform based on the National Instruments (NI) PXI system is built to conduct laboratory experiments including steady-state DC offset, low frequency, and dynamic tests. Finally, the IMFOS is integrated with a GPS-time synchronized distribution level platform, Universal Grid Analyzer (UGA), to demonstrate its applicability for phasor measurement. The Frequency Error (FE) and Total Vector Error (TVE) are explored in an actual distribution level power grid. The contributions are summarized as follows:

- A novel physical displacement-based power grid measuring technology via an IMFOS is presented including both real-time voltage and current sensing. The working principle and the prototype development of the IMFOS are both presented.
- A National Instruments-based characterization platform is set up for performance evaluation.
- To thoroughly compare with existing CTs and PTs, multiple experiments are conducted to verify and evaluate the performance of the IMFOS. The IMFOS is also implemented with a PMU in real-world power systems.

The rest of this paper is organized as follows: Section II provides the principle of voltage and current probe design based on IMFO technology. Section III presents the mechanism of multi-receiving fibers for sensitivity enhancement. Section IV details the IMFOS prototype for distribution power grid sensing. Section V presents the characterization test and UGA implementation to demonstrate the effectiveness of the proposed IMFOS. Finally, the conclusions and potential future research direction are discussed in Section VI.

II. PRINCIPAL OF INTENSITY MODULATED OPTICAL PROBE

In this section, theoretical foundations for the power grid voltage and current sensing via an intensity modulated fiber optic technology are discussed, respectively. The designs of voltage and current probes are given.

A. Voltage sensing

According to the piezoelectric effect, a physical displacement will be induced proportional to the potential difference between two faces of the piezoelectric material [30]. Figure 1 shows the structure of the voltage probe. The power grid voltage V_{in} is divided via the series capacitor C and the piezoelectric transducer. The relationship between the applied voltage V_{in} and the corresponding displacement Δh of the piezoelectric transducer in height can be expressed as

$$\Delta h = crV_{in} \quad (1)$$

where c is the constant piezoelectric coefficient of the piezoelectric transducer and r is the reactance ratio between C and the piezoelectric transducer. According to (1), in response to the applied voltage, the piezoelectric transducer will experience a physical displacement, consequently changing the distance between the fiber probe and the reflective surface of the piezoelectric material.

Figure 1 shows the structure of the voltage probe. To measure the distance, LED light is launched from the Electro-Optic (EO) controller into a transmitting fiber and then bounced back by the reflective surface of piezoelectric material into receiving fibers. The light propagates via the receiving fibers and is detected by the light-sensing end. Then, the power of the received optical light is converted into an electric current by using a photodiode. Finally, an electro-optic circuit is utilized to generate the output voltage, V_{out} , after filtering and amplification. Therefore, the power grid voltage V_{in} , which is proportional to the displacement of the piezoelectric material, is sensed and converted into V_{out} . The parameters of the IMFOS are listed in Table 1.

Table 1 Parameters of the IMFOS

Parameter	Value/descriptions
V_{in} range	1V to 120 V
I_{in} range	1A to 30A
V_{out} range	0V to 5V
Transimpedance gain	5×10^6 V/A
LED emitting wavelength	850nm
Number of the fiber probe	7
Glass core diameter	200 μ m
Plastic cladding	230 μ m
Numerical aperture	0.37
Voltage probe material	PZT-4 piezoceramic (Navy Type I)
Voltage probe size	$12 \times 1.5 \times 0.5$ mm ³
Maximum distance range	500 μ m
Sampling rate	50kHz to 2MHz

B. Current sensing

To sense the current, the IMFOS uses the fiber optic to measure the beam displacement caused by the Lorentz force [31]. Under the Lorentz law, a force F is applied to a charged particle in a perpendicular direction for both the magnetic field and the current, which can be expressed as

$$F = i\mathbf{l} \times \mathbf{B} \quad (2)$$

where B is the flux density, i is the current in the conductor, and l is the length of the conductor.

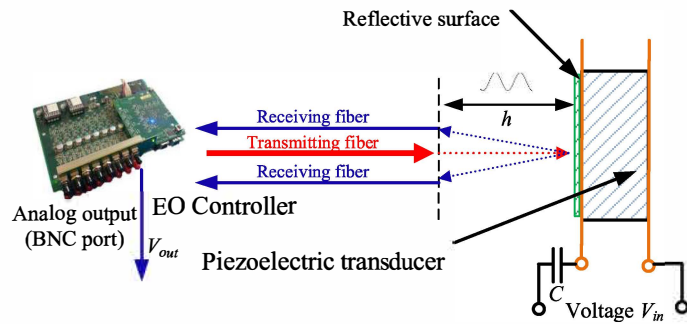


Figure 1. Structure of voltage probe in IMFOS

As shown in Fig. 2, the power grid current I_{in} is split into the shunt and the conductor a , which is placed in a gap in the magnetic core. A force applied to the conductor a can be expressed as

$$F_a = \frac{\mu i_a}{2\pi d} B l \quad (4)$$

where $i_a \ll I_{in}$ and also satisfying $i_a = K_c I_{in}$ where K_c is the current divider coefficient depending on shunt parameters. The force F_a creates a displacement Δy of the conductor beam as

$$\Delta y = \frac{5 F_a L^3}{384 E I} \quad (5)$$

where $\frac{5}{384}$ is a constant that depends on how the beam is mounted. E is the modulus of elasticity of the material from which the beam is fabricated and I is the moment of inertia of the cross-section of the beam. L is the length of the beam. Substituting (4) to (5), we can get

$$\Delta y = \frac{5 \mu I_{in} B l^3 K_c}{384 E I \pi d} \quad (6)$$

It can be seen in (6) that the beam will experience a displacement Δy , which is proportional to I_{in} , towards the direction of the optical probe. Meanwhile, light is launched from the light source into the transmitting fiber and then reflected by the reflective surface of the conductor into the receiving fibers. The light will propagate via the receiving fibers and be detected by the light-sensing end. Therefore, the power grid current I_{in} will be sensed in IMFOS. Then, a similar procedure as discussed in the voltage sensor will be used to convert the receiving optical power into output voltage, V_{out} . The parameters of the current sensor are again listed in Table 1.

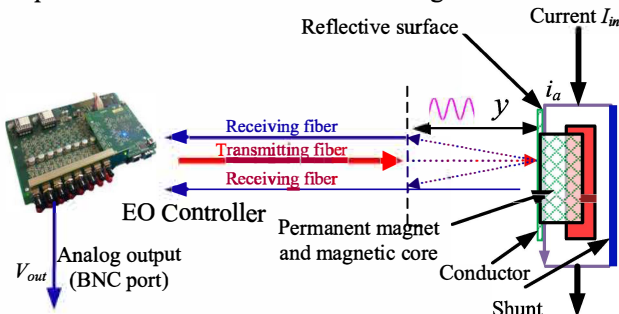


Figure 2. Structure of current probe in IMFOS

III. MULTI RECEIVING FIBERS

To increase the sensitivity of IMFOS, the multi-fiber structure is utilized comprising multiple multimode receiving fibers and one transmitting fiber. The arrangement of the fibers is illustrated in Fig.3. The transmitting fiber is placed in the center of the bundle and is then symmetrically surrounded by multiple of the receiving fibers. All of the fibers are held in a tube, such that the ends of each fiber are adjacent with a distance d to mirror onto transducers exhibiting physical displacement. Because the light is bounced back in all directions on the reflective surface as shown in Fig. 3, the multiple receiving fiber design is beneficial to capture more reflective light and improve the sensitivity.

In the sensitivity test, the fiber is mounted on a micrometer translator, which can be displaced manually against a mirror mounted on the piezoelectric transducer. The PZT 4 cylinder of 2 inch outer diameter and 3 inch length are utilized, which can vibrate in response to the applied voltage. In the test, the probe is manually displaced in a step of $25.4 \mu m$ using the translator. Fig. 4 and Fig. 5 illustrate the comparison between multi-fibers and single-fiber with respect to DC and AC displacement sensitivity over d , respectively. For DC displacement sensitivity, it represents the relationship between reflected light power with the probe-mirror distance. For AC displacement sensitivity, it represents the relationship between signal voltage level and probe-mirror distance. With a higher DC and AC sensitivity, a stronger reflected light and higher voltage of received signal can be obtained, which indicates an enhanced ability to detect the displacement.

According to the results in Fig. 4, the maximum DC sensitivity for one fiber probe occurs at the smallest probe-mirror distance while maximum sensitivity is achieved at a greater distance for the multi-fiber probe. Moreover, a significantly higher light power is detected in the multi-fiber probe. From Fig. 4, the maximum DC displacement sensitivity of the multi-fiber probe is archived in the region of $300-600 \mu m$ with a significantly higher power of detected light. The largest detected light power of a multi-fiber probe is $300 \mu W$ compared to $110 \mu W$ of a single-fiber probe, which indicates the coupler used in the multi-fiber probe increases the detected light power by about 2 times larger than that of a single-fiber probe. It can be seen from Fig. 5 that the maximum AC displacement sensitivity of the multi-fiber probe is approximately 13 dB higher than a single-fiber probe. The increased sensitivity makes a multi-fiber probe a better choice for applications which requires high-quality measurements.

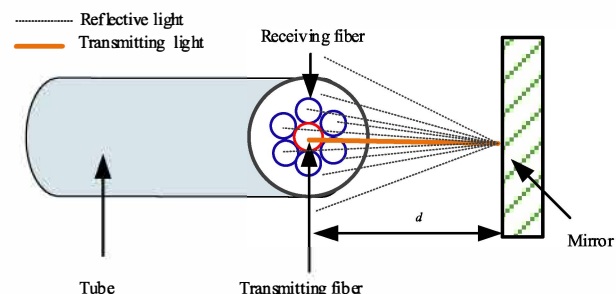


Figure 3. Probe of optical IMFOS

IV. PROTOTYPE DEVELOPMENT

In this section, the prototype of the IMFOS is built for a 120 V/60 Hz distribution power grid. The systematic diagram can be seen in Fig. 6. The maximum and minimum detectable voltages are 120 V and 1 V, respectively. The maximum and minimum detectable voltage are 30 A and 1 A, respectively. The voltage specification is determined by the selection of series capacitor C and piezoelectric transducer while the current specification is determined by the selection of conductor. The IMFOS consists of four major components including a voltage probe, a current probe, an EO controller, and an Aux Processor. A photo of the prototype is shown in Fig. 7. It is noted that there is no mutual influence between the voltage and current probe. For the voltage channel, the physical displacement on the piezoelectric transducer is induced in response to the applied voltage via the piezoelectric effect. For the current channel, the physical displacement occurs on the conductor via Lorentz law. These two displacements are mutually independent of each other and will be captured via two separate optical fiber probes.

the displacement as discussed in Section III. The fiber probe consists of seven identical multimode fibers with a 200 μm diameter glass core and a 230 μm plastic cladding, with a numerical aperture of 0.37. The transmitting fiber is surrounded by multiple receiving fibers distributed in a fixed geometric pattern. For a voltage probe, a bimorph transducer element constructed from PZT-4 piezoceramic (Navy Type I) with nominal dimensions of with nominal dimensions of $12 \times 1.5 \times 0.5$ mm³ are utilized [32]. It is noted that this kind of piezoelectric material has a cantilever resonance frequency around 1.5 kHz. Actually, a variety of geometries can be leveraged with dimensions selection beforehand to realize a predefined resonance frequency considering the tradeoff between the sensitivity and bandwidth. For the current probe, a copper bus bar with a shunt is used as a conductor to pass and divide the current. Voltage drop is taken from the bus-bar via its resistive divider for measurement.

As shown in Fig. 4, the reflected optical power increases with the displacement distance until 500 μm and gradually decreases thereafter. Thus, the quiescent operation point is set at 280 μm with the highest-slope region of the optical response. A photodiode converts the received optical signal into an electric signal in its EO controller. The IMFOS can provide both analog and digital outputs that convert from the optical signal. The analog output is in the range of 0-5 V. On the other hand, the digital output can be accessed via the network interface. The sampling rate can adjust from 50 kHz to 2 MHz. The Aux Processor is a minicomputer with a CentOS7 operating system and an application for digital output visualization as well as the configuration of the IMFOS. Moreover, it will also write the digital output to local files in different data formats including TDMS, LPCM, and MATLAB. The graphical user interface of the application in the Aux Processor can be seen in Fig. 8.

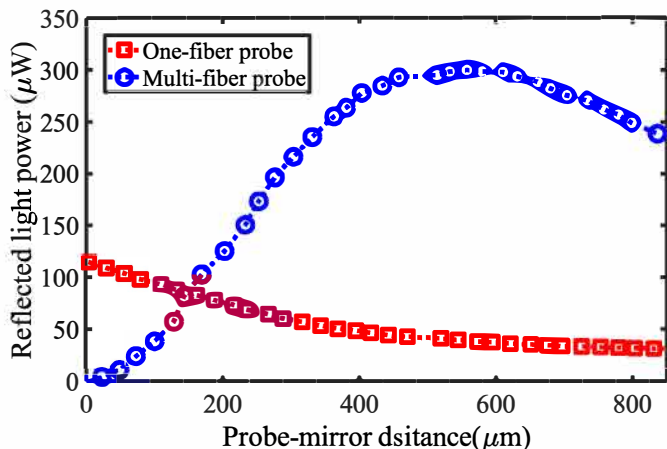


Figure 4. Comparison of DC displacement sensitivity between multi-fiber and one-fiber probes

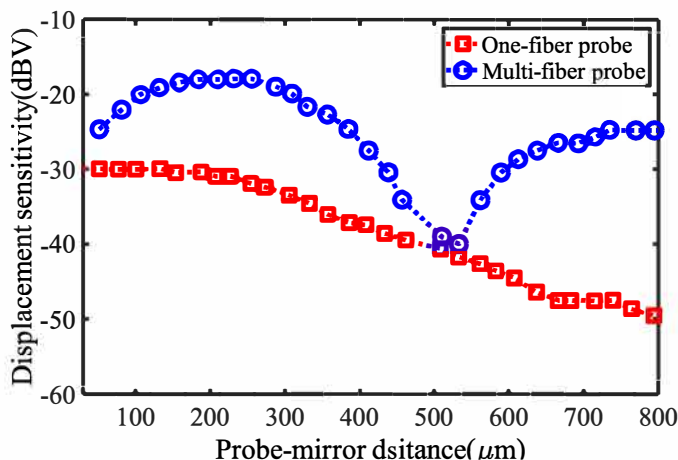


Figure 5. Comparison of AC displacement sensitivity between multi-fiber and one fiber probes

The sensor uses an LED emitting at 850 nanometer wavelengths as a light source with a silicon PIN diode to sense



Figure 6. Diagram of the IMFOS

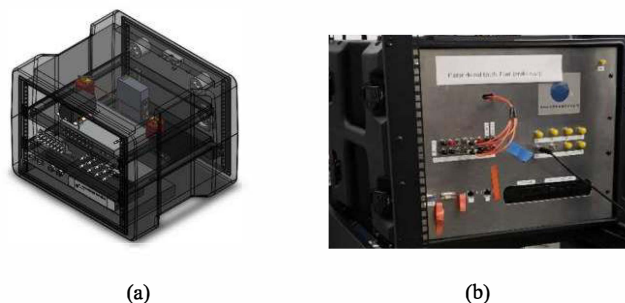


Figure 7. The prototype of IMFOS. (a) Structure perspective drawing (b) Front panel

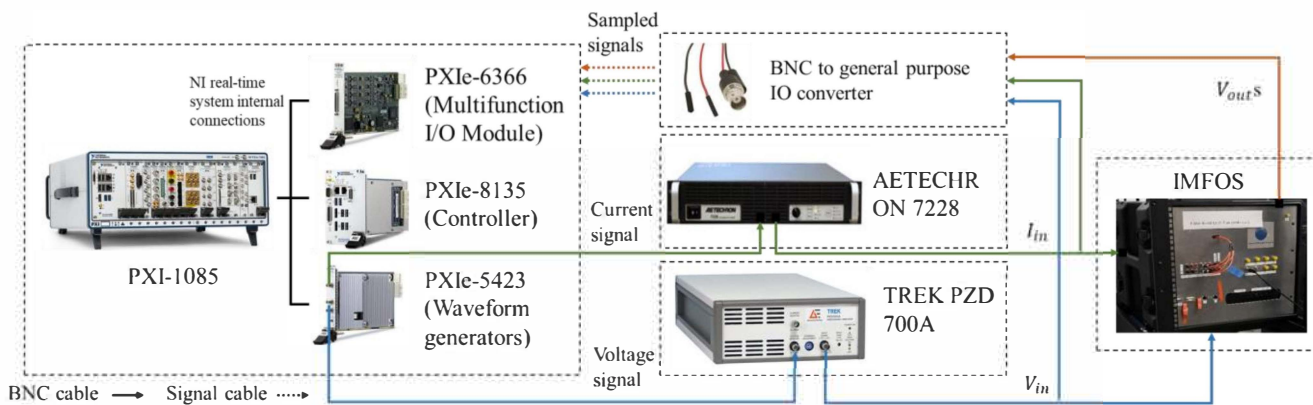
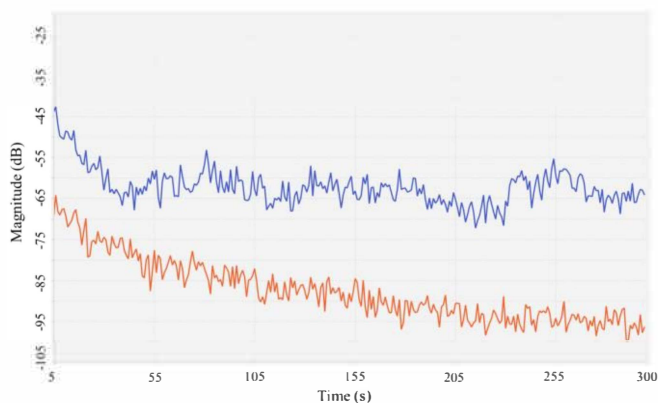
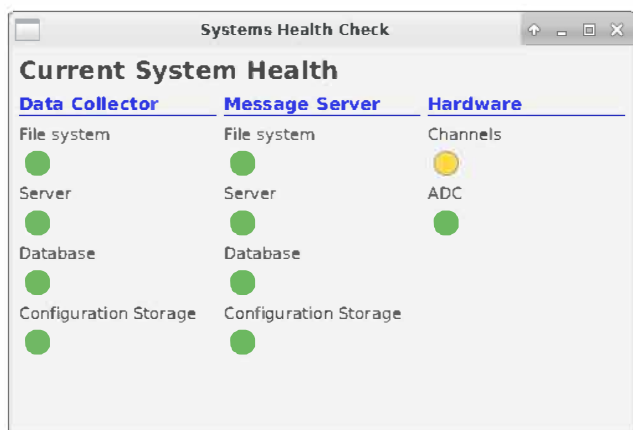


Figure 8. Diagram of the NI based sensor characterization platform



(a)



(b)

Figure 9. GUI of the application in AUX processor
(a) Spectrum of measured signal (b) System configuration.

V. PERFORMANCE EVALUATION

In this section, the performance of the IMFOS is evaluated via the sensor characterization platform and UGA. The diagram of sensor characterization platform is shown in Figure 9. The platform is built using the National Instruments PXI system, which includes an 18-slot PXIe-1085 chassis, an Intel Core i7

embedded controller PXIe-8135, a 40 MHz arbitrary waveform generator PXIe 5423, and a PXIe 6366 with 8 channels of 16-bit ADC. The predefined reference signal is created in a PXIe-8135 and then sent to PXIe 5423 for DA conversion. The output analog signal of PXIe 5423 is then fed into the voltage or the current amplifier for sensor characterization. The TREK PZD 700A and AETECHRON 7228 are utilized as the voltage and current amplifiers, respectively. The output waveforms of amplifiers and sensors under test are simultaneously recorded via PXIe 6366 with 50 kHz sampling rate. As illustrated in Figure 9, since the PXIe-5423, amplifiers, and IMFOS support BNC ports, the voltage and current signals are sent by BNC cables from PXIe-5423 to the amplifier and then to the IMFOS. The output signals from IMFOS are converted to general-purpose signal cables and then received by the PXIe-6366.

A. Steady state test

In the steady state test, the steady sinusoidal signal is generated in NI PXIe 5423 and then fed into the voltage and current amplifiers. The amplitude and frequency response of the IMFOS are tested and the results are shown in Fig. 10. For the amplitude response as shown in Fig.10 (a), by analyzing the amplitude response result, the coefficient of determination R^2 of the linear regression can be calculated as,

$$R^2 = 1 - \frac{\sum_i (V_i - f_i)^2}{\sum_i (V_i - \bar{V})^2}, \quad (7)$$

where V_i and f_i are the voltage fitted values at index i . \bar{V} is the mean of voltage measurements. In the best case, the voltage values match the fitted values so that R^2 is equal to 1. R^2 of the current measurement can be calculated in the similar method. Illustrated in Fig.10 (a), the R^2 is larger than 0.99, which demonstrates the high linearity of the IMFOS. For the frequency response, it is discovered that the IMFOS has a flat region from 10 Hz to 1000 Hz, illustrated in Fig.10 (b). The overall spectral characteristic of the prototype is impacted by various factors including piezoelectric/conductor material, low pass filter in its EO controller, transmitting fiber, fiber mounting strategy. The effective frequency response range can be defined as the frequencies with amplitudes above the flat region, i.e, 10 Hz to 3000 Hz. The narrow frequency range is

one disadvantage of the proposed sensor. To improve it, one potential solution is to apply an effective filter to filter out the resonant region of the transducer.

B. DC offset and low frequency test

The DC and low frequency test is conducted by comparing the magnetic CT and PT, since the magnetic core transducer is susceptible to DC and low frequency injection. The Agilent 6812B and Omicron CMC256 are used to produce voltage and current signals, respectively, in this subsection. First, a 60 Hz sinusoidal waveform superposed with a 20% DC component is generated. From the result in Fig. 11 and Fig. 12, the saturation effect caused by the DC component can be observed in the output of the magnetic transducer while no negative impact is found for the IMFOS, which demonstrates DC immunity in IMFOS. From the Fig.11(b) and Fig. 12 (b), the magnetic PT and CT have severe 2nd and 3rd harmonic distortions, which make their output unreliable under this circumstance. Thus, the IMFOS outperforms the magnetic based sensor when the input signal has a DC offset, which could be caused by various factors such as geomagnetic disturbance, transient grounding fault or EMTP3 [12][29]. Fig. 13 shows the results of the low frequency test. A 14.5 Hz sinusoidal frequency component is injected into the sensors under test. Similarly, a severe distortion can be seen for magnetic PT and CT while the saturation effect is successfully eliminated in IMFOS, indicating that the low frequency signal can be accurately measured by utilizing the optic-electric technology. To have a quantitative comparison among the IMFOS, PT, and CT, the voltage and current errors under three test cases are listed in Table 2. It can be clearly observed that the voltage errors of the IMFOS are as low as those of the PT under both DC offset and low-frequency tests. However, the current errors of the IMFOS are much lower than those of CTs under two test cases. These results indicate that the voltage measurement accuracy of the IMFOS is as good as PTs while the current measurement accuracy is better than CTs under DC offset and low-frequency test cases.

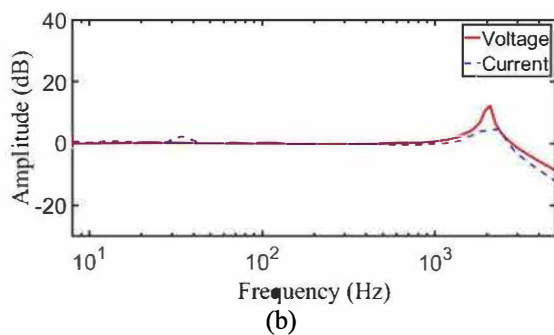
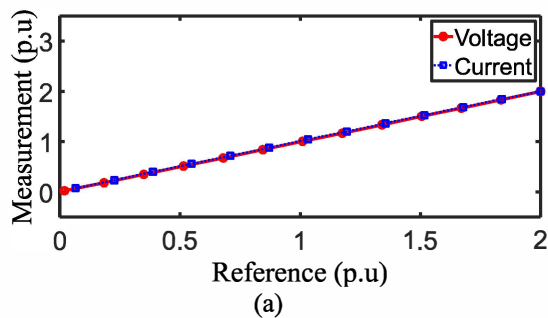


Figure 10. Result of steady state test (a). Amplitude response (b). Frequency response

Table 2 Comparison among IMFOS, PT, and CT

Test cases	IMFOS		Frequency error	PT		CT	
	Voltage error	Current error		Voltage error	Current error		
DC offset test	0.0532 p.u.	0.0036 p.u.	NA	0.0559 p.u.	0.1347 p.u.		
Low-frequency test	0.0277 p.u.	0.0065 p.u.	NA	0.0619 p.u.	0.2331 p.u.		
Dynamic test	0.00059 p.u.	0.0011 p.u.	2m Hz	NA	NA		

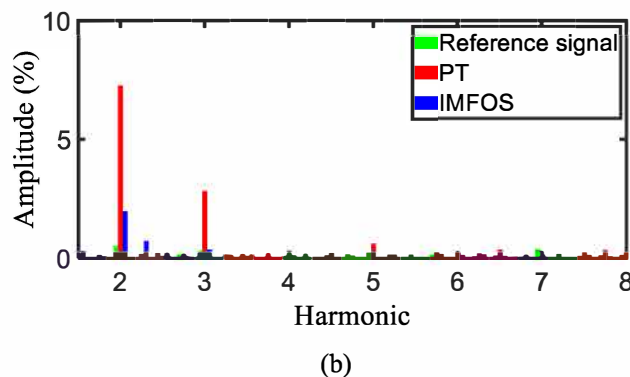
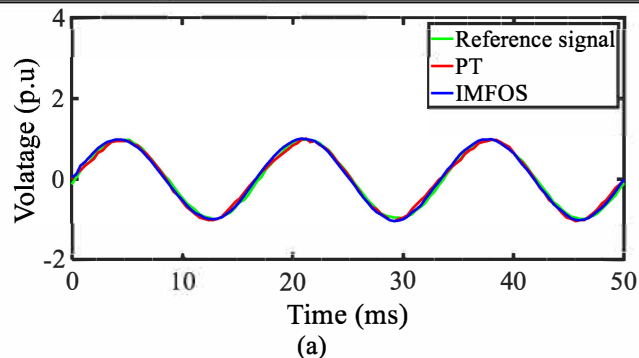


Figure 11. Voltage test with DC component. (a). Time-domain waveform (b). Harmonic and inter-harmonic components

C. Dynamic Test

The aim of the dynamic test is to assess the capability of the IMFOS for capturing the dynamic behavior of the input signal. Step change and ramp for the amplitude and frequency are tested referring to IEEE C37.118 standard [33]. For the frequency step change test, the frequency of the input signal jumps up from 60 Hz to 61 Hz, stays at 61 Hz for 2 seconds, and then jumps back down to 60 Hz. For the frequency ramp test, the frequency of the input signal first ramps up from 59.5 Hz to 60.5 Hz in 2 seconds at a rate of 0.5 Hz/s, stays at 60.5 Hz for 2 seconds, then ramps down from 60.5 Hz to 59.5 Hz in 2 seconds at a rate of -0.5 Hz/s. The amplitude dynamic tests employ similar change characteristics as the frequency dynamic tests. The testing results are shown in Fig.14 and Fig.15. The recursive discrete Fourier transform is adopted for the frequency calculation and the root mean square is calculated to obtain voltage and current amplitude. From the results, the reference signal and output of IMFOS match well, which

verifies the ability of the IMFOS to track the dynamic behavior of signals. Again, a quantitative analysis of the IMFOS is listed in Table 2 under the dynamic test. The results show that both the voltage and current measurements are very precise under dynamic tests. In addition, the average frequency error is 2m Hz which is lower than the PMU frequency measurement requirement under a frequency ramp test listed in the IEEE C37.118.1[33].

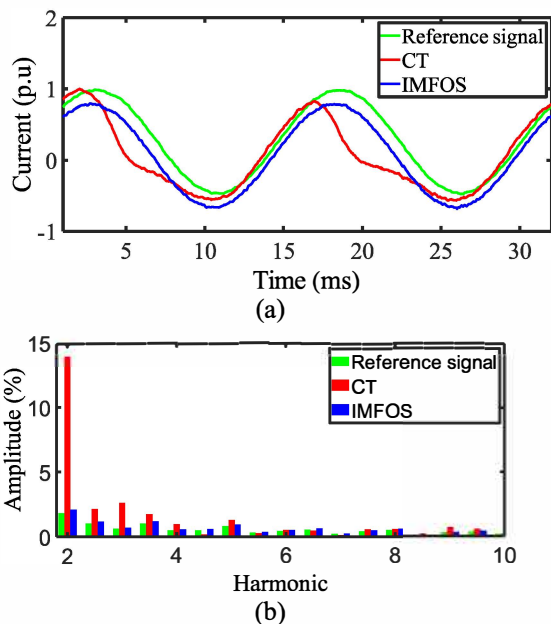


Figure 12. Current test with DC component. (a)Time-domain waveform (b) Harmonic and inter-harmonic

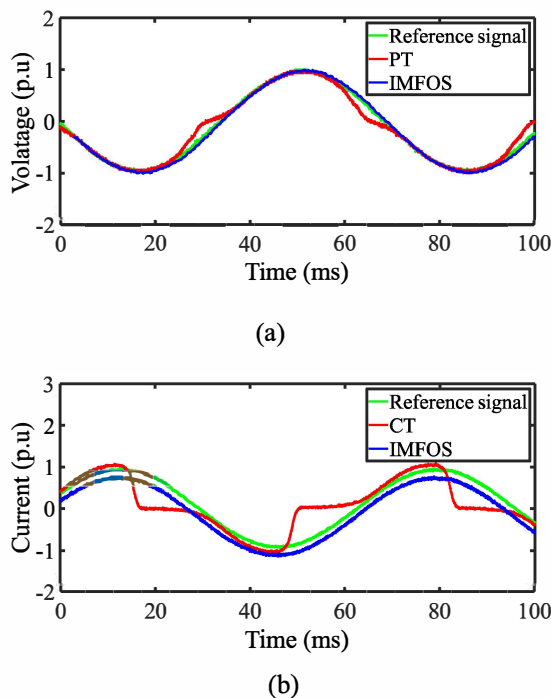


Figure 13. Test results with low frequency (14.5Hz) component. (a) Voltage test. (b) Current test

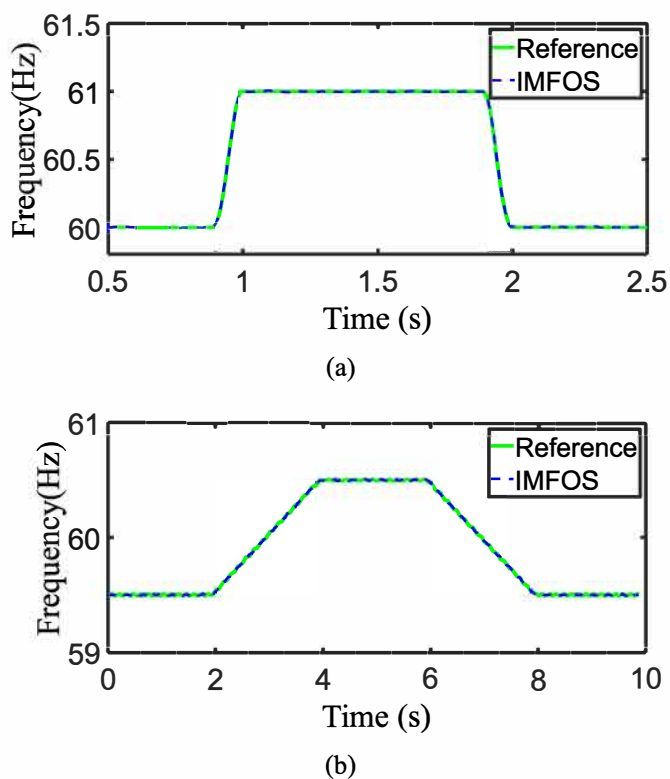


Figure 14. Frequency dynamic test. (a) Voltage frequency step change (b) Current frequency ramp

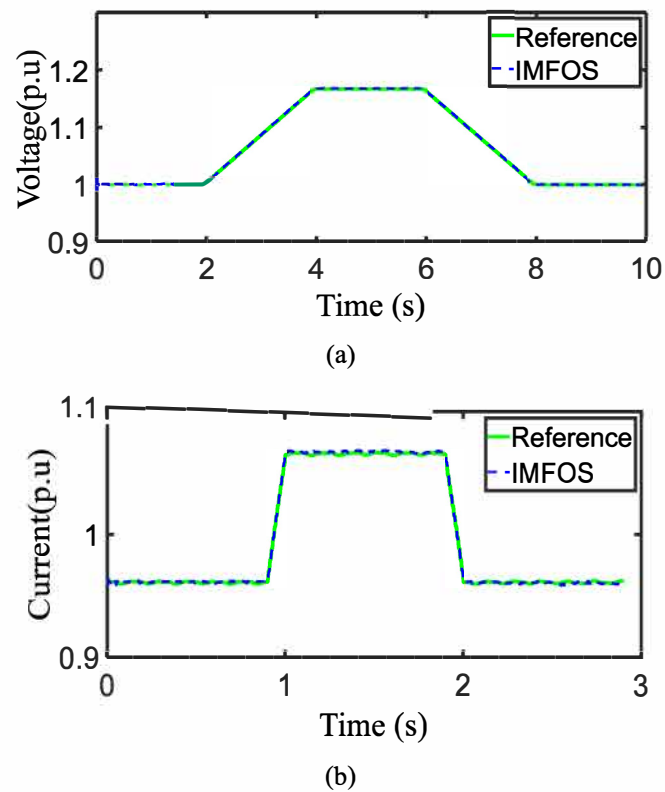


Figure 15. Amplitude dynamic test. (a) Voltage amplitude ramp (b) Current amplitude step change

D. Implementation in Universal Grid Analyzer

To demonstrate the applicability of IMFOS for phasor estimation in an actual power grid, the IMFOS is implemented in the Universal Grid Analyzer platform, referred as IMFOS-UGA, as shown in Fig. 16. The IMFOS is connected to a distribution power grid and provides input signals to a UGA for synchronized frequency, angle, and magnitude measurements. For the sake of comparison, a normal UGA with accuracies of 1m Hz for the frequency, 0.05V for the voltage magnitude, and 0.05° for the angle is set up as a reference. The two UGAs are time-synchronized by GPS signal throughout the test; thus, the measurements can be aligned with the UTC timestamp. The results of the frequency, angle, and voltage magnitude measurements are shown in Fig. 17 (a)-(c). It can be seen in Fig. 17 that the IMFOS-UGA has the capability to synchronously capture the trends of its frequency, angle, and amplitude over time. The FE and TVE are as small as 2m Hz and 0.029%, which are sufficient to comply with the 5mHz and 1% requirement of the IEEE PMU standard C37.118.1 [33]. It is worth mentioning that UGA is utilized as an example platform for synchronized power grid monitoring. Since the output analog signal of the sensor is 0~5V DC, it is easily integrated with any other kinds of existing power grid measurement devices such as phasor measurement units and power quality analyzers for repeatable tests.

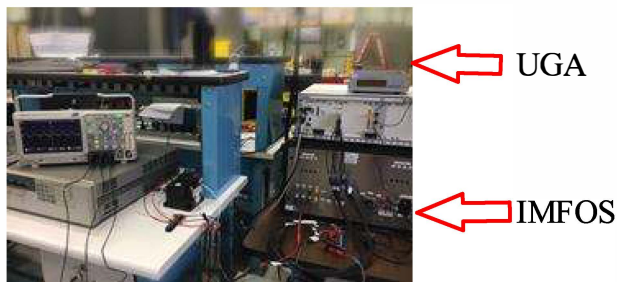


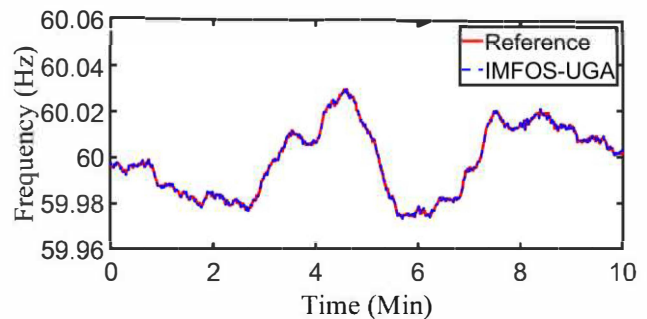
Figure 16. Test setup for UGA implementation

VI. CONCLUSION

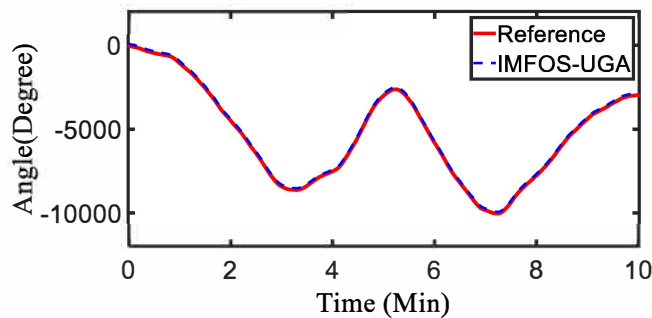
In this paper, the IMFOS was developed to monitor grid voltage and current via the measurement of the physical displacement of transducers caused by the piezoelectric effect and the Lorentz-force with the advantage of simplicity. The intensity modulated fiber optic light is transmitted to the transducers via a one center fiber and reflected by the mirrors in the transducers. Then multiple multimode fibers symmetrically surrounding the center fiber with enhancement sensitivity are exploited to collect the reflected signal to its EO controller. A prototype was built to demonstrate the feasibility; its performance was evaluated via a NI based characterization platform under conditions of both steady and dynamic states, DC, and low frequency interferences. Experimental results demonstrated its linearity and ability to capture dynamic changes for measured voltage and current signals. This also verified its merit for DC and low frequency immunity compared to the conventional magnetic PT and CT, indicating that the IMFOS would be a promising tool for electric grid monitoring. Lastly, the prototype of IMFOS was implemented

in the UGA platform to demonstrate its applicability for distribution power grid phasor monitoring. The FE and TVE of the IMFOS-UGA met the 5m Hz and 1% requirement outlined in the IEEE PMU C37.118 standard.

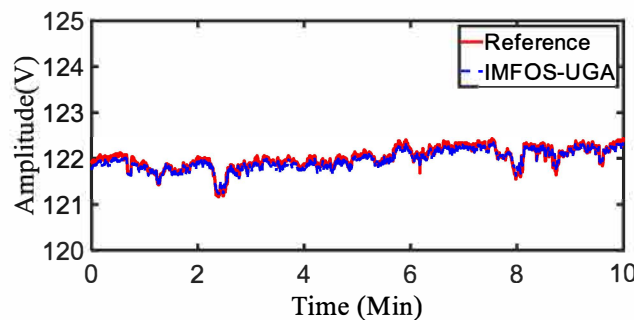
It is noted that the major elements of the IMFOS, including LED, fiber, conductor, piezoelectric material, and copper busbar, are commonplace. With high-volume production in mind, the cost of the IMFOS will no doubt be competitive with conventional PT and CT. Future research will focus on noise reduction and robustness improvement. Penitential solutions include: 1) Integration of an effective filter to filter out the resonant region and low frequency noise. 2) Temperature compensation for the whole electro-optic system.



(a)



(b)



(c)

Figure 17. Test result for IMFOS-UGA. (a) Frequency (b) Angle (c) Amplitude

REFERENCES

- [1] Z. Li, H. Liu, J. Zhao, T. Bi and Q. Yang, "A Power System Disturbance Classification Method Robust to PMU Data Quality Issues," in *IEEE Trans Industrial Informatics*, vol. 18, no. 1, pp. 130-142, Jan. 2022, doi: 10.1109/TII.2021.3072397.

- [2] J. Zhang, H. Wen and L. Tang, "Improved Smoothing Frequency Shifting and Filtering Algorithm for Harmonic Analysis With Systematic Error Compensation," *IEEE Trans Industrial Electronics*, vol. 66, no. 12, pp. 9500-9509, Dec. 2019.
- [3] Y. Cui, F. Bai, R. Yan, T. Saha, R. K. L. Ko and Y. Liu, "Source Authentication of Distribution Synchrophasors for Cybersecurity of Microgrids," in *IEEE Trans. Smart Grid*, vol. 12, no. 5, pp. 4577-4580, Sept. 2021, doi: 10.1109/TSG.2021.3089041.
- [4] W. Wang et al., "Frequency Disturbance Event Detection Based on Synchrophasors and Deep Learning," *IEEE Trans. Smart Grid*. DOI: 10.1109/TSG.2020.2971909
- [5] Y. Cui et al., "Multifractal Characterization of Distribution Synchrophasors for Cybersecurity Defense of Smart Grids," in *IEEE Trans. Smart Grid*, doi: 10.1109/TSG.2021.3132536.
- [6] S. Liu et al., "Data-Driven Event Detection of Power Systems Based on Unequal-Interval Reduction of PMU Data and Local Outlier Factor," *IEEE Trans. Smart Grid*, vol. 11, no. 2, pp. 1630-1643, March 2020.
- [7] A. Alsabbagh, B. Wu and C. Ma, "Distributed Electric Vehicles Charging Management Considering Time Anxiety and Customer Behaviors," in *IEEE Trans Industrial Informatics*, vol. 17, no. 4, pp. 2422-2431, April 2021, doi: 10.1109/TII.2020.3003669.
- [8] K. Sun et al., "WAMS-based HVDC Damping Control for Cyber Attack Defense," in *IEEE Trans. Power Systems*, doi: 10.1109/TPWRS.2022.3168078.
- [9] Zhu L, Zhao Y, Cui Y, You S, Yu W, Liu S, Yin H, Chen C, Wu Y, Qiu W, Mandich M. Adding power of artificial intelligence to situational awareness of large interconnections dominated by inverter - based resources. *High Voltage*. 2021 Dec;6(6):924-37.
- [10] Liu S, Zhao Y, Lin Z, Liu Y, Ding Y, Yang L, Yi S. Data-driven event detection of power systems based on unequal-interval reduction of PMU data and local outlier factor. *IEEE Trans. Smart Grid*. 2019 Sep 16;11(2):1630-43.
- [11] A. G. Phadke and J. S. Thorp, "Synchronized Phasor Measurements and Their Applications," *Power Electronics and Power Systems*, 2017.
- [12] IEEE Guide for the Application of Current Transformers Used for Protective Relaying Purposes," in *IEEE Std C37.110-2007 (Revision of Std C37.110-1996)*, vol., no., pp.1-90, 7 April 2008
- [13] G. Franceschini, E. Lorenzani and G. Buticchi, "Saturation Compensation Strategy for Grid Connected Converters Based on Line Frequency Transformers," *IEEE Trans. Energy Conversion*, vol. 27, no. 2, pp. 229-237, June 2012.
- [14] IEEE Recommended Practice for the Application of Instrument Transformers in Industrial and Commercial Power Systems," *IEEE Std 3004.1-2013*, vol., no., pp.1-48, 6 May 2013
- [15] W. Yao and et al, Utilization of optical sensors for phasor measurement units, *Electric Power Systems Research*, vo. 156, pp.12-14, 2018,
- [16] P. Niewczas and J. R. McDonald, "Advanced Optical Sensors for Power and Energy Systems Applications," *IEEE Instrum Meas Magazine*, vol. 10, no. 1, pp. 18-28, Feb. 2007.
- [17] W. Yao and et al, "Pioneer Design of Non-Contact Synchronized Measurement Devices Using Electric and Magnetic Field Sensors," *IEEE Trans. Smart Grid*, vol. 9, no. 6, pp. 5622-5630, Nov. 2018.
- [18] W. Yao, H. Lu, M. J. Till, W. Gao and Y. Liu, "Synchronized Wireless Measurement of High-Voltage Power System Frequency Using Mobile Embedded Systems," *IEEE Trans. Industrial Electronics*, vol. 65, no. 3, pp. 2775-2784, March 2018.
- [19] E. Udd and W. B. Spillman Jr, eds., *Fiber Optic Sensors: An Introduction for Engineers and Scientists*, Wiley, New York, NY, 2011.
- [20] K. Bremer et al., "Fibre optic pressure and temperature sensor for geothermal wells," *SENSORS*, 2010 IEEE, Kona, HI, 2010, pp. 538-541.
- [21] Li, J., Liu, H., Bi, T. and Zhao, J., 2020. Second-order matrix pencil-based phasor measurement algorithm for P-class PMUs. *IET Generation, Transmission & Distribution*, 14(19), pp.3953-3961.
- [22] H. Wang, C. Zhuang, R. Zeng, S. Xie and J. He, "Transient Voltage Measurements for Overhead Transmission Lines and Substations by Metal-Free and Contactless Integrated Electro-Optic Field Sensors," *IEEE Trans. Industrial Electronics*, vol. 66, no. 1, pp. 571-579, Jan. 2019.
- [23] Z. Li, H. Liu, J. Zhao, T. Bi and Q. Yang, "A Power System Disturbance Classification Method Robust to PMU Data Quality Issues," in *IEEE Trans. Industrial Electronics Informatics*, vol. 18, no. 1, pp. 130-142, Jan. 2022, doi: 10.1109/TII.2021.3072397.
- [24] W. Sima, R. Han, Q. Yang, S. Sun and T. Liu, "Dual LiNbO3 Crystal-Based Batteryless and Contactless Optical Transient Overvoltage Sensor for Overhead Transmission Line and Substation Applications," *IEEE Trans. Industrial Electronics*, vol. 64, no. 9, pp. 7323-7332, Sept. 2017.
- [25] S. Xu, H. Liu and T. Bi, "A Novel Frequency Estimation Method Based on Complex Bandpass Filters for P-Class PMUs With Short Reporting Latency," in *IEEE Trans. Power Delivery*, vol. 36, no. 6, pp. 3318-3328, Dec. 2021, doi: 10.1109/TPWRD.2020.3038703..
- [26] R. Daniel, Monitoring electrical assets for fault and efficiency correction, United States Patent, No. 7714735,2006
- [27] N. Lagakos, V. Kaybulkin, P. Hernandez, and C. Vizas, Fiber optic electromagnetic phenomena sensors, U.S. Patent 9,823,277, 2017.
- [28] T. Lan, C. Zhang, S. Fu, B. Zhu, M. Tang and W. Tong, "Spatial Division Multiplexing-Based Reflective Intensity-Modulated Fiber Optics Displacement Sensor," *IEEE Photonics Journal*, vol. 10, no. 4, pp. 1-7, Aug. 2018, Art no. 7103707.
- [29] W. Yao and et al, Magnetic field based wireless gmd/emp-e3 impact monitoring device, US.Patent, publicaiton NO. 20180136267
- [30] Z. Wu, "A Wide Linearity Range Current Sensor Based on Piezoelectric Effect," *IEEE Sensors Journal*, vol. 17, no. 11, pp. 3298-3301, 1 June, 2017.
- [31] D. Roylance, Beam Displacements., Department of Materials Science and Engineering, MIT, pp. 1-12, 2000.
- [32] U.S. Department of Defense, MIL-STD-1376B(SH), 1995.
- [33] *IEEE Standard for Synchrophasor Measurements for Power Systems*, IEEE Standard C37.118.1-2011, Dec. 2011



Wenxuan Yao (SM'20) received the B.S. from the College of Electrical and Information Engineering, Human University, Changsha, China, in 2011 and the Ph.D. degree from the Department of Electrical Engineering and Computer Science, University of Tennessee, Knoxville, TN, USA, in 2018.

He is currently a Professor with Human University. He was a Research Associate with Oak Ridge National Laboratory from 2018 to 2020. His research interests

include wide area monitoring system, PMU application, embedded system development, power quality, and big data analysis in power systems.



Lingwei Zhan (M'15) received the B.S. and M.S. degrees in electrical engineering from Tongji University in 2008 and 2011, respectively. He received his Ph.D. degree in the Department of Electrical Engineering and Computer Science at the University of Tennessee, Knoxville, in 2015. He is currently a R&D staff with Oak Ridge National Laboratory.

His research interests include advanced grid monitors, PMU, synchrophasor measurement algorithms, wide-area power system monitoring, renewable

energy sources, FACTS, and HVDC..



Sterling Sean Rooke received his engineering Ph.D. from University of Maryland College Park and is a researcher within the Electrical Engineering Department of the University of Tennessee Knoxville. As an entrepreneur, Dr. Rooke leads both X8 LLC and Brixon, Inc. as they advance cyberspace technologies including machine learning informed industrial controls. As a reserve military officer, Rooke advises the U.S. Government and Air Force in the areas of cyber and technology matters. Rooke was previously an active duty Information Warfare officer in the

United States Navy where he was the command SBIR lead and assigned to IARPA. Previously as a civilian, Dr. Rooke focused on optics, wireless, and electromechanical packaging concerns. His early laboratory research was in the area of polymer chemistry and biotechnology. Previously Dr. Rooke was the Communications Division Director for ISA and a Instrumentation Measurement Chapter Chair for IEEE.

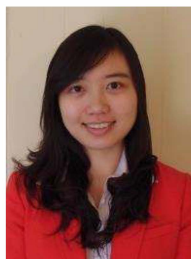
Christopher Vizas received the B.A. and J.D. from the Yale University, USA, in 1971 and 1975, respectively. He is now the Chairman at Smartsensecom Inc.

Victor Kaybulkin received the M.S. from the Department of Electronics and Radio Wave Physics, Lobachevsky State University of Nizhny Novgorod - National Research University, Russia. He is now a Sr. scientist at Smartsensecom Inc. His research interests are Fiber-optic sensors research, design, and development.



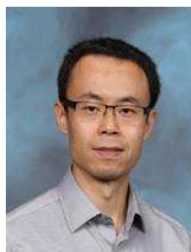
Thomas J. (Tom) King received the B.S. degree in mechanical engineering from Clarkson University, Potsdam, NY, USA, the M.S. degree in materials engineering from Rensselaer Polytechnic Institute, Troy, NY, USA, and the business degree from the University of Tennessee, Knoxville, TN, USA. He has a dual role with the Oak Ridge National Laboratory (ORNL), Oak Ridge, TN, USA, and the University of Tennessee. He is the Director of the Sustainable Electricity Program with ORNL, where he is responsible for leading, coordinating, and

implementing ORNL's research and development portfolio of projects conducted for the U.S. Department of Energy (DOE)'s Office of Energy Efficiency and Renewable Energy and Office of Electricity Delivery and Energy Reliability. He is the Director of Industry and Innovation with University of Tennessee for the jointly funded NSF-DOE Engineering Research Center, CURENT.



Bailu Xiao (Member, IEEE) received the B.S. and M.S. degrees in electrical engineering from Huazhong University of Science and Technology, Wuhan, China, in 2006 and 2008, respectively, and the Ph.D. degree in electrical engineering from the University of Tennessee, Knoxville, TN, USA, in 2014.

She is a R&D staff at Oak Ridge National Laboratory (ORNL). Her current research interests include power electronics system integration, multilevel converters, and microgrid modeling and control.



Zhi Li (Member, IEEE) received the B.S.E.E. and M.S. degrees in electrical engineering from Tsinghua University in 2000 and 2003, and the Ph.D. degree in electrical engineering from Washington State University. He is a research group leader at the Sichuan Energy Internet Research Institute, Tsinghua University. He was with the U.S. Department of Energy's Oak Ridge National Laboratory as a postdoctoral research associate and then a R&D staff member from 2012 to 2022.

His research areas include power system analysis, electromagnetic fields modeling and analysis for power grid applications, and high voltage engineering.



Yilu Liu (F'04) received her M.S. and Ph.D. degrees from the Ohio State University, Columbus, in 1986 and 1989. She received the B.S. degree from Xian Jiaotong University, China.

Dr. Liu is currently the Governor's Chair at the University of Tennessee, Knoxville and Oak Ridge National Laboratory (ORNL). Dr. Liu is elected as the member of National Academy of Engineering in 2016. She is also the deputy Director of the DOE/NSF-cofunded engineering research center

CURENT. Prior to joining UTK/ORNL, she was a Professor at Virginia Tech. She led the effort to create the North American power grid Frequency Monitoring Network (FNET) at Virginia Tech, which is now operated at UTK and ORNL as GridEye. Her current research interests include power system wide-area monitoring and control, large interconnection-level dynamic simulations, electromagnetic transient analysis, and power transformer modeling and diagnosis.



He Yin (S'13-M'16-SM-22) received the B.S. and Ph.D. degree in the electrical and computer engineering from University of Michigan-Shanghai Jiao Tong University Joint Institute, Shanghai Jiao Tong University, Shanghai, China in 2012 and 2017, respectively. He is currently a research assistant professor at Center for Ultra-Wide-Area Resilient Electric Energy Transmission Networks (CURENT), University of Tennessee, Knoxville, TN, USA.

His research interests include optimization and decentralized control of microgrid, PMU design, and power system situational awareness.